17 August 2020. Version for NORA of the paper published
in the African Journal of Marine Science
https://doi.org/10.2989/1814232X.2020.1776390

Wave Setup at Tristan da Cunha

Philip L. Woodworth

National Oceanography Centre, Joseph Proudman Building, 6 Brownlow Street, Liverpool L3 5DA, United Kingdom

Correspondence to: P.L. Woodworth (plw@noc.ac.uk)

Abstract

Wave setup is investigated using data from tide gauges in a small harbour at the island of Tristan da Cunha in the South Atlantic Ocean. Frequent examples of wave setup were found during the period 1986-1992, but were much less apparent after 1992, following extensions to the two breakwater arms of the harbour. The unambiguous association of wave setup with the several decimetre spikes in Tristan sea level, which can persist for a day or so, are a warning that signals related to wave setup could also occur in other tide gauge records, where the wave setup signal could perhaps be misinterpreted as wind setup within the overall storm surge. One conclusion is that, in spite of the difficulties of access to Tristan and its ever-present hostile wave climate, the island is undoubtedly now worthy of a permanent tide gauge installation that would be an important contribution to the global sea level network.

Keywords: Wave and wind setup; Tide gauge measurements; Sea and land level monitoring; High-frequency sea level variability

Introduction

Tide gauge records are used by many researchers to study ocean processes that result in a change in the level of the sea. Such processes include ocean tides, storm surges and seasonal and long-term changes in mean sea level (Pugh and Woodworth 2014). In some cases, there are positive ‘spikes’ (i.e. transient increases in sea level) superimposed on the tidal curves which occur during periods with large ocean waves. These spikes can span many hours to days and have a magnitude of decimetres or sometimes over 1 metre. They result from a process called wave setup in which wave breaking and dissipation raise water levels in the surf zone, with the size of the spikes being typically 25% of the adjacent deep-water significant wave height (SWH) (e.g. Bowen et al. 1968, Vetter et al. 2010, Becker et al. 2014). [1] In many cases, the waves contain a large component due to swell produced by distant storms (Hoeke et al. 2013, Dodet et al. 2019). A different type of wave setup can occur in enclosed harbours with entrances exposed to incoming wave energy (Thompson and Hamon 1980, McDougal and Slotta 1981, Thompson 1983).

Wave setup is usually considered to be an undesirable feature of a sea level record. Its importance to a long-term sea level station record can sometimes be reduced by relocating the tide gauge to a different position in the port or along the coast. Nevertheless, an operator often has no choice of exact gauge location, which can depend primarily on practicalities such as access to mains electrical power or site security (IOC 2016). Therefore, it is important to learn as much as possible about this process by studying records in which the wave setup signal is clearly identified. That is why locations such as Tristan da Cunha which have little or no continental shelf are particularly interesting. In these cases, the non-tidal (storm surge) component of the record will have almost no contributions from wind setup, which enables the wave setup component to be studied unambiguously.

This paper describes how wave setup is manifested in a small enclosed harbour at Tristan da Cunha, the entrance of which is exposed almost continuously to energetic waves arriving primarily from the west but sometimes from a more northerly direction or occasionally even from the northeast or east. We also demonstrate how the spikes of several decimetres in the tide gauge record associated with wave setup in the earlier part of the record were much reduced when the enclosing arms of the harbour entrance were extended into deeper water.

Tristan da Cunha is an active volcanic island at approximately 37 °S , 12 °W in the South Atlantic Ocean with almost no areas of coastal shelf and with water depth exceeding 50 m within 100 m of some parts of the coast. Its only settlement is called Edinburgh of the Seven Seas, on the northwest corner of island, close to where the eruption of 1961 occurred (Figure 1a). Crawford (1982) describes how the islanders were evacuated to England following the eruption and how most of them returned in 1963. The eruption had destroyed the former landing beaches but had created a new lagoon just below the settlement. The islanders themselves were responsible for the construction of a new harbour out of the lagoon, the bottom of which had to be blasted out in places. Two breakwater arms were constructed on reefs to the east and west of the former lagoon using ‘gabions’, plastic-coated wire

[1] This process is usually referred to as ‘static wave setup’ which is appropriate for discussion of tide gauge data with 10-minute or similar averaging of sea level such as that discussed in this report; higher-frequency oscillations associated with ‘dynamic wave setup’ and the ‘infragravity waves’ first identified by Walter Munk could also occur (Dean and Walton 2009).

baskets packed with stones and boulders and covered in cement. After a while, it was necessary to provide reinforcement to the breakwater arms from attack by the sea by adding piles of ‘dolosses’ to the seaward side of each one. A dolosse is a double-anchor-shaped concrete block that links together with its neighbour to form a strong coastal defence.

Calshot Harbour, named after the Hampshire village where the islanders stayed in England, opened in January 1967. It has a diameter of approximately 50 m and an entrance that is 15 m wide and approximately 2.5 m deep (Figure 2a,b,c and see below). It has proved to be a great asset, particularly for offshore fishing activities. However, it is exposed to energetic waves that usually arrive from the west. As noted by Crawford (1982), wave conditions have interfered with harbour operations ever since its construction, and even with the extensions to the breakwater arms described below, the harbour remains unusable on many days in the year (e.g. Figure 2c). Occasionally, waves impinge on the harbour from a more northerly direction and it will be shown that these occurrences are especially important with regard to wave setup.

Bouton et al. (2016) mention that by 1990 small seaward extensions had been built on both breakwaters. In addition, they refer to the more significant extensions to the two breakwater arms made in 1992-1994, using dolosses weighing 1.8-3.5 tonnes, along with a deepening of the harbour basin, resulting in what is essentially the present-day harbour. Further harbour refurbishments took place in 2008-2009. The western breakwater was damaged in a major storm in August 2010, necessitating reinforcing of a structure that is continuously under attack by waves. Bouton et al. (2016) provide details of those repairs. The research associated with that project included the construction of a physical model (Kieviet et al. 2016) and the collection of as much information as possible concerning the bathymetry of the harbour and adjacent waters. Some of that information was made available for the present study.

For example, in a survey by Robin Webb Consulting Ltd. dated 1999, the depth of the harbour entrance is shown as 2 m below Lowest Astronomical Tide (Chart Datum), decreasing to ~1 m inside the harbour and even shallower in its southeast corner. Almost the same impression comes from a chart compiled by WSP/Parsons Brinckerhoff in 2010 (Figure 1b). However, another made in 2017 by WSP suggests that harbour depths had been increased by ~1m throughout, in particular with a deepening of the southeast corner, such that the harbour now has an approximately uniform depth. It is difficult to determine changes in the average depth from one survey to another due to what appear to be uncertainties in datum. Nevertheless, it is clear that harbour depths must have gradually increased through the years.

We are not aware of a survey of harbour bathymetry between its construction in the mid-1960s until the one in 1999. One can find remarks that the harbour basin was deepened on occasions. For example, Bouton et al. (2016) state that it was deepened between 1992 and 1994. However, the details are not clear. Nevertheless, one would have thought that the depths during the 1980s to early 1990s (the period of most interest below with regard to the wave setup spikes) cannot have been very different from those shown in the 1999 and 2010 surveys.

The photograph in Figure 2c provides a good view of the harbour from its eastern side and looking approximately north-west (TdCG/RSPB 2012). It shows clearly the extensions to the breakwaters, especially the western breakwater, made around 1992. It also provides a good demonstration of wave breaking near to the harbour. Although the weather was fine on this day, the sea was rough and no fishing was possible. Waves can be seen breaking outside the harbour in water depths of ~10 m or less, while other breaking is occurring at the harbour entrance where the depth is ~3 m. There is also some over-topping of the eastern breakwater. From ERA-Interim satellite information discussed below, we know that deep-water SWH around Tristan was very large at this time (~ 8.5 m) and, as a general rule, waves will break when they enter water depths less than 1.3 times their SWH (Pugh and Woodworth 2014), which is qualitatively consistent with the wave breaking in the photograph.

As mentioned above, Calshot Harbour is exposed at most times to waves arriving from the west, and it is primarily those persistent conditions which cause most of the damage to the armoured sections of the breakwaters. Kieviet et al. (2016) explain how shallow reefs to the west of the harbour result in shoaling and refraction at the head of the western breakwater. They provide an example of such activity during a storm in June 2006. From ERA-Interim, we know that wave direction at the time of the photograph in Figure 2c was also from slightly south of west. However, it will be shown below that it was the relatively infrequent occasions of large SWH arriving from a more northerly direction that were responsible for the observed wave setup spikes in the sea level record prior to 1992.

Materials

Bottom Pressure and Island Tide Gauge Data during the Tristan Triangle Experiment

In the late 1980s, an experiment was conducted at, and around, Tristan da Cunha to investigate how changes in sub-surface pressure (SSP) measured by an island tide gauge differed from changes in SSP measured in the nearby deep ocean. The island tide gauge was an 'absolute' pressure sensor with the recorded SSP variations being due to either changes in sea level or in atmospheric pressure (aside from any changes due to variations in ocean water density). In addition, three bottom pressure recorders (BPRs) were deployed at the corners of a triangle around the island in order to measure deep-ocean SSP. The BPRs were located approximately 200 km from Tristan da Cunha, at positions to the NE, W and SE of the island, and at depths of between 3100 and 4100 m (see Figure 1a of Hughes and Smithson 1996). The SSP time series from the three sites were found to be very similar, and were used subsequently by Hughes and Smithson (1996) in a study of the spatial scales of SSP variability in this part of the South Atlantic.

Figure 3 shows the time series of SSP from the three BPRs and from the island tide gauge for the one year for which all three BPRs were deployed simultaneously and the island gauge was operational. (Individual BPR time series are available before and after this period but this was the only time that all three were deployed successfully together). The BPR data were in the form of hourly integrations of pressure, while the island tide gauge record consisted of 15-minute integrations that were averaged further into hourly values. Digiquartz absolute pressure sensors were used in almost all of these deployments and in those discussed below. For present purposes, changes in SSP measured in mbar can be taken as corresponding to changes in sea level in centimetres.

Each SSP hourly time series was subjected to a tidal analysis to remove the small astronomical tide; the largest constituent (M2, the main lunar semidiurnal tide) has an amplitude of only 0.22 m (Cartwright et al. 1988). Then, the residuals of the tidal analysis were averaged into 10-hour means, following the procedure used by Hughes and Smithson (1996). It is these 10-hour residuals that are plotted in Figure 3. Ten hours might seem a long averaging period for study of changes in SSP due to wave setup. However, because of the long duration of storms, findings on setup are much the same whether one uses 1- or 10-hour residuals; this aspect is discussed further below.

To a good approximation, the three BPR records are identical (see Hughes and Smithson 1996 for a discussion of this topic). The important thing for present purposes is to note that there are differences between the island tide gauge record and those of the BPRs. For example, SSP in the tide gauge record has a slightly different seasonal cycle to those of the BPRs, as might be expected if there are different seasonal changes in water properties in the shallow and deep ocean. More importantly, the island record also contains several positive spikes of 20-30 cm in May and July-September (relative to the average over the year), unlike the BPR time series which contain no spikes. Therefore, as such positive spikes never occur due to ocean dynamics (or at least that part of it that is forced by meteorology, see below), one can conclude that the spikes in harbour SSP must have been due to waves through either wave setup and/or over-topping of the harbour arms. Further evidence for this interpretation is provided below.

Island Tide Gauge Data 1986-1992 and 1992-1997

The history of the Tristan harbour tide gauge is a long and not always successful one, with the earlier sensors sometimes subject to instrumental drift and environmental challenges. (Extensive growth of kelp is a major problem for instruments such as pressure sensors deployed underwater.) Figure 4 shows the extended record of SSP, with the end of each separate deployment indicated by a triangle.

The original records were mostly in the form of 15-minute integrations of SSP, although they were sometimes 7.5- or 30- minute, or one-hour, integrations. They were all acquired from sensors located at the same position on the east side of the harbour. As a first step, all of them were averaged further into hourly means and processed individually as described above. The mean SSP during an individual record was subtracted from the resulting 10-hour average residuals before plotting in Figure 4.[2]

A first observation is that there is a low-frequency component of SSP of the order of ± 5 mbar which is much reduced after 1992. We believe that the variability before 1992 is primarily an artefact of the instrumental difficulties at that time. (There is some similarity between the SSP from the island tide gauge during 1986-1988 and that obtained from Geosat altimetry. However, the Geosat record is not long or accurate enough to provide a better comparison. Only weak correspondence was found

[2] Aside from the wave setup of interest to the present study, it is possible that the Tristan harbour experiences high-frequency sea level variability due to seiches. However, any seiches would have periods of several 10s of seconds for which the sampling of the available tide gauge data is inadequate. We are informed (Mr. Robin Webb, private communication) that the harbour also sometimes demonstrates the clapotis effect whereby reflections of waves from a harbour wall result in standing wave patterns; we have no way of commenting on the possibility of those wave-related processes either.

between measured SSP and that of ocean models, indicating the difficulty for models to represent ocean variability in this area or, more likely, the instrumental difficulties.) Nevertheless, this low-frequency variability is not large enough to hide the fact that positive spikes of several tens of mbar (i.e. several decimetres of sea level) are present many times through the time series up to 1992, similar to those described above for 1986-87. If one defines a spike by a threshold of either 20 or 25 mbar, then one finds that 40 % of them occur during the winter months of July-September, although in fact a spike can occur in any month.

Much had been learned by 1992 concerning the operation of pressure sensors at South Atlantic locations, including at Tristan. Accurate tide gauges called 'B gauges' containing three pressure sensors (Woodworth et al. 1996, IOC 2002) had been developed for use at other South Atlantic locations, and were also tested at Tristan where they were less successful because of the smaller tidal range. In practice, the sub-surface sensors in the Tristan B-gauges were used to continue the earlier harbour measurements of SSP.

The low-frequency variability in this later period can be seen to be much smaller than before, and is in fact a reliable measurement of the ocean's real low-frequency variability in SSP, as shown in Figure 4 by comparison to observations from space by the 'reference series' of precise satellite altimetry missions which commenced in 1992 (the TOPEX/POSEDON and JASON missions, shown by the blue time series in Figure 4). The fact that an improvement in tide gauge measurements happened at the same time as the start of precise altimetry was not a coincidence. This was the start of the World Ocean Circulation Experiment, in which altimetry was an essential component, and new tide gauges were being deployed around the world to provide a validation of the altimeter information (Spencer et al. 1993, Woodworth et al. 2002). Of course, 1992 was also the time of the breakwater extensions, and Figure 4 shows that there were few decimetric spikes in this later period after 1992 except on odd occasions in 1996 and 1997.

Later Island Tide Gauge Data 2011-2013

After a long gap, a new OTT RLS (Radar Level Sensor) radar tide gauge was installed in the harbour in February 2011, in the same position as the earlier pressure sensors. It operated until June 2011, by which time the gauge had clearly developed a fault. The gauge was replaced by another OTT RLS in November 2012 which operated until May 2013 when it was hit by a boat. These experiences demonstrate how radar sensors are vulnerable to damage when located in a small, busy harbour.

The record for 2011-2013 comprised 1-minute values of sea level which were averaged into 15-minute and hourly means. Air pressure values from the National Centers for Environmental Prediction (NCEP) - National Center for Atmospheric Research (NCAR) reanalyses (Kalnay et al. 1996, Kistler et al. 2001, https://www.cdc.noaa.gov) were added assuming 0.9948 cm/mbar in order to convert sea level into what is effectively SSP. The hourly record was then subjected to a tidal analysis and residuals inspected for any evidence of spikes such as those described for the SSP data up to 1992. Two clear examples were found: one spanning 5-6 July 2011 (approximately 35 cm) and another in the morning of 19 May 2012 (approximately 50 cm) (Supplementary Figure 1a,b).

Aside from a small number of cases such as these, the general absence of spikes in the island tide gauge data for 1992-1997, and in this more recent data for 2011-2013, implies that the harbour record can be regarded now as being essentially free from wave setup effects, and therefore that Tristan can now be considered as good a location for measuring sea level with tide gauges as most other places. The SSP time series derived from the radar gauge data, expressed as daily values, is shown in Figure 5. While some contribution from the two large events mentioned above propagates into the daily values, the time series can be seen to be very similar to information from satellite altimetry. For completeness, one should state that the data from the two radar sensors should have been adjusted for instrumental range bias that could be different for each sensor. Unfortunately, the sensors were deployed before range calibration could be checked. However, the biases are likely to be the similar (to within perhaps ~1 cm) in instruments from the same manufacturer.

Results

(Non-)Association of the Spikes with Atmospheric Forcing

Figure 3 showed that there were no spikes in SSP in the BPR measurements in the deep ocean adjacent to Tristan during 1986-1987. In fact, one can demonstrate that spikes are unlikely ever to be found in SSP over the deep ocean near Tristan by using information from the Dynamic Atmosphere Correction (DAC) model. The DAC model is used extensively by the altimetry community and can be obtained from the Archivage, Validation et Interprétation des données des Satellites Océanographiques (AVISO) web site (https://www.aviso.altimetry.fr). It simulates the dynamical changes in sea level that occur at all points in the ocean due to air pressure changes and winds by using a high-resolution barotopic model for high-frequency variability (timescales less than 20 days) and an assumption of the inverse barometer (IB) response for longer timescales (Carrère and Lyard 2003). (Ocean variability with periods of 12 and 24 hours corresponding to those of the S2 and S1 atmospheric tides is not included in the DAC fields, see the above AVISO web site; this aspect is not important with regard to their use here.) Model outputs are provided every 6 hours on a 0.25° global grid.

Any measurements of SSP by a sub-surface pressure sensor will represent a combination of: (1) the changes in air pressure above the sensor, (2) the static response of sea level to those changes in air pressure (the 'IB effect'), and (3) the sea level changes due to the ocean's dynamical response to changing meteorological conditions (e.g. Hirose et al. 2001). Consequently, (1) and (2) compensate each other automatically in the SSP record and, if that record contains spikes, then, in this scenario, they can arise only from the dynamical contributions (3).

In most ocean areas, one might expect the dynamics to be important at short timescales (e.g. several hours to several days). However, this seems not to be the case in the ocean around Tristan. One can compare the DAC values at Tristan to the purely-IB values that can be computed from 6-hourly fields of surface air pressure obtained from NCEP. We define these 'pure-IB' values in terms of (minus) the local air pressure anomaly. For example, for the period 1993-1997 one obtains a standard deviation of differences between DAC and pure-IB values of only 2.7 cm, together with the suggestion of a small seasonal cycle (Figure 6). Similarly, the period 2011-2013 has a standard deviation of 2.8 cm. The seasonal cycle in the differences will be due to that in air pressure averaged over the global ocean (Wunsch and Stammer 1997); it is unimportant to the present discussion. The DAC and NCEP meteorological products will inevitably differ slightly because of different data processing. Therefore, Figure 6 probably provides a slight over-estimate of the differences between DAC and purely-IB values that one would compute using products from the same meteorological centre. Figure 6 demonstrates that SSP at this point in the ocean, but outside the harbour, will contain no spikes due to the high-frequency dynamics that last 10 hours or longer and have a magnitude of more than a few cm. Consequently, any decimetric spikes in SSP actually observed in the island tide gauge record must be due to other processes, local to Tristan, such as those related to waves discussed below.

Association of the Spikes with Wave Setup

A next step is to investigate how the spikes in the sea level record relate to wave conditions at Tristan, using 6-hourly wave information from the ERA-Interim data set of the European Centre for Medium-Range Weather Forecasts (ECMWF) (Dee et al. 2011). We consider first the earlier period 1986-1992 with its many positive spikes, and use a more sophisticated method to define their magnitude. To do this we make use of 1-hour instead of 10-hour residuals, and instead of simply subtracting the mean SSP for the record, we subtract the mean SSP in a window ± 7 days either side of the residual in question but not including ± 1.5 days either side. The ± 7 days was selected in order to obtain an estimate of the low-frequency background in SSP around the time of the residual, while the ± 1.5 days was chosen in order to not bias that background SSP estimate by including similarly large residuals occurring during the same storm at approximately the same time as the residual in question.

Of course, the 1-hour residuals used here are larger than the 10-hour residuals described above, but they are not different to any great extent because the events of wave setup span an extended period of a day or so (i.e. the duration of a storm). Figure 7 provides an example. Because the events last so long, and because the tidal range at Tristan is so small, there can be little dependence of wave setup on high or low tide.

Figure 8(a) shows a histogram of SWH at times closest to the times of each residual during 1986-1992. The distribution can be seen to peak at approximately 2.2 m and have an average of 2.9 m with a long tail out to 6 m or so. Wave direction is normally around 240° (i.e. from approximately WSW) (Figure 8b), and wave period is about 9 seconds (Figure 8c). However, there are occasions when this normal situation does not apply. Selecting times of spikes larger than 25 cm (419 1-hour values) results in SWH values centred at about 5 m, wave direction about 320° (i.e. from the NW) and a slightly longer wave period (Figure 8d-f).

One arrives at the same conclusions in the reverse direction by identifying the residuals associated with certain wave conditions. Figure 9(a) shows a histogram of the residuals for all wave conditions during 1986-1992; this is necessarily centred on zero but with a longer tail on the positive side. However, selecting the 5% of times with large waves (SWH > 4 m) and from a more northerly direction (270° - 45°), results in residuals that are almost all positive and with a long tail out to 60 cm or more (Figure 9b). These figures demonstrate conclusively that the spikes in the SSP record during 1986-1992 were associated with large waves from a northerly direction.

Using ERA-Interim data for 1993-1997 results in similar histograms of SWH etc. to those in Figure 8(a-c), as shown in Supplementary Figure 2(a-c). Also, by selecting the very few large spikes in the SSP residuals during 1993-1997 (only 11 1-hour values larger than 25 cm), one arrives at the same conclusions derived from Figure 8(d-f) i.e. that spikes are associated with large SWH from a more northerly direction (Supplementary Figure 2(d-f)). In fact, these were unusually energetic events with SWH values of 4-8 m. In these later 5 years (1993-1997), large northerly waves occurred 6% of the time (i.e. the number of entries in Supplementary Figure 3b compared to Supplementary Figure 3a), approximately as frequently as during 1986-1992 (i.e. the number of entries in Figure 9b compared to Figure 9a), so the much smaller number of spikes during 1993-1997 cannot be accounted for by a different wave climatology. (One may also note that, discussion of very large residuals aside, the distributions of Supplementary Figure 3(a,b) are wider than those of Figure 9(a,b), representing the generally noisier data in the earlier years, cf. Figure 4).

The fact that the spikes during 1986-1992 were associated with unusual wave conditions at almost any time during the year (although, as mentioned above, 40% of them occurred during July-September) can also be demonstrated by fitting annual cycles in SWH, wave direction and period to the entire ERA-Interim data set. For example, Figure 10(a) plots 6-hourly SWH for 2011-2013, to which an average annual cycle has been fitted, demonstrating an average of 3.0 m, and an annual amplitude of ~0.6 m peaking in mid-July. Values of 5 m or more are therefore unusual at any time of year. Wave direction is 244° on average with a less apparent annual amplitude of only ~5° peaking in October (Figure 10b). Therefore, waves with a direction of 320° are similarly unusual. Wave period (Figure 10c) has an average of 9.4 seconds and an annual amplitude of ~0.3 seconds peaking in late-June. (These findings are consistent using information for either 1986-1997, or for the 2011-2013 data shown in Figure 10).

As for the two spikes on 5-6 July 2011 and 19 May 2012 during the radar data of 2011-2013, in both cases ERA-Interim data demonstrates that waves with SWH of about 6 m impinged on the harbour from the northeast or east (the former from approximately 20° E of N, the latter from about 75° E of N). Comparison to Figure 8(a,b), for example, demonstrates that these were very unusual events indeed, in which the western breakwater extension would have provided no shelter at all. (The latter event was during the most violent easterly storm since that of 23 May 2001, during which unfortunately we had no operational tide gauge, see https://www.tristandc.com/newsstorms2006-12.php.)

Discussion

The preceding sections have shown that the observed spikes in SSP in Tristan harbour are not due to dynamical changes in sea level in the nearby deep ocean arising from atmospheric forcing. If one had been discussing a tide gauge on a coastline next to a wide continental shelf, then its record could have also contained signals from local wind setup, which will appear similar to the signals from wave setup, as the two components of a storm surge will have similar timescales set by the duration of the storms (e.g. Kim et al. 2010, Bertin et al. 2015, Pedreros et al. 2018). Of course, the two processes can be estimated separately by means of additional instrumentation and/or numerical modelling. However, they cannot be separated from an inspection of tide gauge residuals alone. That is why Tristan, with its absence of continental shelf and therefore of the wind setup component of the storm surge, was of particular interest for the present study, as the only possible reasons for the spikes in this case must be related to waves. However, there are several mechanisms by which waves could be responsible.

When waves propagate into shallow water in the direction of a coast with a sloping bottom, their amplitudes increase through shoaling until they become unstable and break (Dean and Walton 2009). Figure 2(c) shows an example. Sometimes the waves are in the form of ocean swell that could have travelled considerable distances (e.g. Aucan et al. 2012, Hoeke et al. 2013). The reduction in wave energy due to breaking leads to a radiation stress gradient, with momentum transferred from waves to the water column (Longuet-Higgins and Stewart 1962, Bowen et al. 1968, Holman and Sallenger 1985, Stockdon et al. 2006, Dean and Walton 2009, Woodworth et al. 2019). Assuming steady-state conditions, the radiation stress gradient is balanced by higher water levels at the shore which is the wave setup.

To a good approximation, the wave setup that occurs due to waves arriving normal to the coast, or nearly normal (e.g. 30° from normal), depends only on SWH and is independent of the gradient of the bottom slope (Dean and Walton 2009). The elevated water levels associated with setup can be an appreciable proportion (20-30%) of the incident deep-water SWH (e.g. Becker et al. 2014) although examples with proportions in the wide range 10-200% have been reported (Dodet et al. 2019). Therefore, there are locations where setup can be as large as ~1 m (e.g. Aucan et al. 2012). In these cases, wave setup will usually last for a day or so, and will contribute to the computation of the monthly mean values of sea level that are used for climate studies (e.g. Melet et al. 2016).

In the present case of Tristan, Kieviet et al. (2016) explained how the waves that arrive at the harbour from the west nowadays undergo shoaling on the reefs to the west of the harbour and refract around the western breakwater into the entrance. One suspects that something similar occurred prior to 1992, before extra protection was provided by the western breakwater extension. In either case, wave heights would have been reduced by the time waves entered the harbour and no large spikes should have occurred. In these cases, we also suspect that waves would have been responsible for a long-shore pressure gradient that can drive a local circulation (Dean and Walton 2009).

However, In the case of waves arriving more from the north, almost normal to the north coast of Tristan and almost directly into the pre-1992 harbour, then one can picture wave setup being present along that entire short section of coast resulting in an increase in sea level of at least 10% of the offshore SWH, as in the several examples of wave setup at other locations mentioned above. Consequently, the observation of spikes in the tide gauge record of the order of 40-50 cm is quite plausible. As long as the large waves in question (e.g. SWH > 4 m) broke outside the harbour, then the wave setup observed by a gauge in the harbour should have been similar to that at any point on that section of coast. In practice, the complicated hydrodynamics associated with the real bathymetry and coastline, including the harbour, could well have modified the magnitude of the wave setup spikes.

We must next consider changes in wave setup due to breaking waves outside the harbour after the western extension was made in 1992. That extension will have closed off the harbour to much of the energy of waves arriving from the west, although by no means all of that energy as Kieviet et al. (2016) demonstrated. In addition, its curved shape, which was probably dictated by the shape of the reef on which the breakwater rests, must now also obstruct wave setup from the surf zone to the coast for waves from more northwestern or northerly directions. Therefore, given that the end of the western extension is only a short distance from the breaking waves (Figure 2c), it is unsurprising that there should have been a reduction in the number of large spikes.

It is also of interest to consider another possibility for the spikes, in this case for a harbour with waves impinging on its entrance, as discussed by Thompson and Hamon (1980). They argued that as waves spread into a harbour from a narrow entrance, their amplitude decreases. No wave breaking occurs in this case. Radiation stress arguments can then be used to calculate the steady-state wave setup for large, long-period waves at distances within the harbour greater than a few times the width of the entrance. McDougal and Slotta (1981) discussed how wave diffraction at the entrance of such a harbour would result in wave setup varying with distance from the entrance (see also Mehta 1990). They also noted that setup would depend on water depth during the tidal cycle (which is not important for Tristan). Wave setup away from the entrance is given by $0.75a^2/h$ where a^2 is the water level variance due to waves at the entrance and h is the depth of the harbour. One can take $SWH = 4a$ from which it follows that:

$$Setup = (0.75/16)SWH^2/h$$

[1]

Thompson (1983) found that this approach provided a satisfactory explanation of data obtained at Sydney Harbour, a considerably larger harbour than at Tristan where wave reflections in the small harbour will necessarily invalidate the simple picture of spreading wave fronts as in the model. Nevertheless, one can make a calculation along these lines for Tristan with h = 1.5 m and SWH = 4 m (i.e. in the upper tail of the distribution in Figure 8a). Then the wave setup will be ~0.5 m, which is the order of magnitude of the spikes in Figure 4 before 1992.

However, this is a less plausible explanation for the Tristan spikes given that, in practice, we know that wave breaking will have begun outside the harbour, and that the SWH of waves at the entrance will be less than 4 m. In addition, Tristan has a much smaller harbour than Thompson and Hamon (1980) were considering. Consequently, this does seem to be a useful model to apply to an explanation of the elimination of spikes after 1992 when the extensions to the breakwater arms were made and the harbour was deepened by some amount. If we take h = 2.5 m after 1992 (i.e. a deepening of the harbour after 1992 by an average of 1.0 m), then Equation (1) suggests that setup should have been reduced by ~40%. This does not seem to be enough.

A third way to picture what has been and is now happening at Tristan is to think of the breakwaters as akin to the reefs of Pacific coral islands where the first research into wave setup was made (Munk and Sargent 1948, Tait 1972). At times of very high wave setup, there could be spikes in the harbour tide gauge record due to flows over the top of the breakwaters into the harbour, the breakwaters having a height of only ~2 m above the still water level. There is also a possibility of water forced through gaps in the breakwaters. Then the water return flow would be impeded by the narrow harbour entrance (akin to narrow gaps in a reef) resulting in 'pumping up' of the harbour. In this scenario, the amount of overtopping, the change in harbour area, and modifications to its entrance would all have been different before and after 1992.

Conclusions

Clearly, all of the above suggestions for the origin of the wave setup spikes are speculative and can only be confirmed by detailed wave modelling using either numerical or physical methods. Nevertheless, some such explanation is needed to account for the observed changes before and after 1992. Whatever the real explanation, the information presented here demonstrates the relative importance of waves arriving from the north. It would be interesting to undertake further research in order to understand the origins of northerly waves in particular events. In addition, the present study has shown from the data before and after 1982 just how sensitive the wave-related content of a sea level record can be to the local harbour arrangement. The findings are a lesson to anyone planning a new tide gauge installation, or moving a gauge from one position to another, to choose if possible an optimal location for minimising all wave-related effects (IOC 2016). Such a choice of location was never available to us at Tristan.

For many years, Tristan was thought to be desirable in principle, although impractical in practice, as a location for a tide gauge station that was part of the Global Sea Level Observing System (GLOSS) (IOC 2012). This reservation was primarily due to the difficulty of access to the island, which explains why Tristan has had a long, although very gappy, tide gauge record. There were also the harsh wave conditions to consider, which resulted in a preference for the use of pressure sensor tide gauges. However, after the first data had been collected, an additional concern arose about the value of the data, given the observation of the occasional large spikes. They suggested that the harbour tide gauge might not always provide a reliable monitor of the open-ocean sea level variability required for oceanographic research. However, the spikes only ever comprised ~1-2% of the hourly record and their exclusion from the record would have affected the monthly mean values of SSP by only several tenths of a mbar (several mm of sea level), even for the period with many spikes during 1986-1992 in Figure 4. However, now that we clearly understand the reason for them, we can readily filter them from the data set if necessary given supplementary knowledge of wave conditions from ERA-Interim, for example.

Therefore, a conclusion from the present study is that the harbour modifications in 1992 must have resulted in Tristan now being no worse than some other locations in GLOSS as regards wave setup. Consequently, although other reservations remain to some extent, Tristan should be recognised as an important remote location that is suitable for all kinds of environmental monitoring, including the measurement of sea and land levels for GLOSS. In particular, the later data in Figure 4 demonstrate that a Tristan harbour tide gauge is perfectly capable of recording the open-ocean sea level variability of interest to ocean circulation and climate change research. Therefore, Tristan deserves to have a well-maintained tide gauge that can be included in the South Atlantic contributions to the global network. We are pleased that a new radar tide gauge was installed at Tristan in December 2017 and we hope that recording at this location can now be maintained in the long term.

Acknowledgements

I am grateful to my colleagues in the National Oceanography Centre who deployed the tide gauges and BPRs at Tristan da Cunha over many years. These included Bob Spencer, Peter Foden, Jeff Pugh and Ian Vassie, and our laboratory Director, Dr. David Cartwright FRS, who had the original idea for the Tristan Triangle experiment. These deployments would not have been possible without the help of the Tristan islanders. Collaboration at Tristan da Cunha with the University of Luxembourg (Norman Teferle and Dietmar Backes) is also much appreciated, and they are thanked for the topographic information in Figure 1a.

Paul Bouton from WSP/Parsons Brinckerhoff in Cape Town and Robin Webb of Robin Webb Consulting Ltd. kindly supplied detailed information on harbour improvements and coastal bathymetry. The bathymetric information in Figure 1(b) is the property of the Tristan da Cunha Government. Sean Burns, the Administrator of Tristan da Cunha, and Katrine Herian from the Royal Society for the Protection of Birds were of great help regarding the timing of the photograph in Figure 2(c). I thank Chris Hughes for the satellite altimeter data from the reference series of missions and for DAC data and ocean model information. Richard Ray from the Goddard Space Flight Center provided Geosat altimeter data. I am grateful for advice on wave setup from Mark Merrifield and Judith Wolf. All the tide gauge and BPR data used in this paper may be obtained from https://www.ntslf.org/files/acclaimdata or from the author. Figure 1(a) was generated using the Generic Mapping Tools (Wessel and Smith 1998).

Author ORCID ids

Philip L. Woodworth, ORCID: 0000-0002-6681-239x

References

Aucan J, Hoeke R, Merrifield MA. 2012. Wave-driven sea level anomalies at the Midway tide gauge as an index of North Pacific storminess over the past 60 years. *Geophysical Research Letters* 39:L17603, doi:10.1029/2012GL052993.

Becker JM, Merrifield MA, Ford M. 2014. Water level effects on breaking wave setup for Pacific Island fringing reefs. *Journal of Geophysical Research-Oceans* 119:914-932, doi:10.1002/2013JC009373.

Bertin X, Li K, Roland A, Bidlot JR. 2015. The contribution of short-waves in storm surges: two case studies in the Bay of Biscay. *Continental Shelf Research* 96:1–15, doi:10.1016/j.csr.2015.01.005.

Bouton P, van Eeden F, Retief M, De Roubaix F, Kieviet J. 2016. Emergency repairs to the main breakwater of Calshot Harbour on Tristan da Cunha island. pp.1515-1529 in, Proceedings of 35th International Conference on Coastal Engineering (ICCE 2016), Antalya, Turkey 17-20 November 2016 (ed. P. Lynett). ISBN 9781510844087. Los Angeles: International Conference on Coastal Engineering (ICCE).

Bowen AJ, Inman DL, Simmons VP. 1968. Wave 'set-down' and set-Up. *Journal of Geophysical Research* 73(8):2569-2577, doi:10.1029/JB073i008p02569.

Carrère L, Lyard F. 2003. Modeling the barotropic response of the global ocean to atmospheric wind and pressure forcing - comparisons with observations. *Geophysical Research Letters* 30:1275, doi:10.1029/2002GL016473.

Cartwright DE, Spencer R, Vassie JM, Woodworth PL. 1988. The tides of the Atlantic Ocean, 60N to 30S. *Philosophical Transactions of the Royal Society of London A* 324:513-563, doi:10.1098/rsta.1988.0037.

Crawford A. 1982. *Tristan da Cunha and the roaring forties.* Edinburgh: Charles Skilton Ltd. 256pp.

Dean RG, Walton TL. 2009. Wave setup. Chapter 1 (pp. 1-23) in, *Handbook of Coastal and Ocean Engineering.* (ed. Y.C. Kim). World Scientific Publishing Co. Ltd. http://www.worldscibooks.com/engineering/6914.html.

Dee DP, Uppala SM, Simmons AJ, Berrisford P, Poli P, Kobayashi S, Andrae U, et al. 2011. The ERA-Interim reanalysis: configuration and performance of the data assimilation system. *Quarterly Journal of the Royal Meteorological Society* 137:553–597, doi:10.1002/qj.828.

Dodet G, Melet A, Ardhuin F, Bertin X, Idier D, Almar R. 2019. The contribution of wind generated waves to coastal sea level changes. *Surveys in Geophysics* 40:1563-1601, doi:10.1007/s10712-019-09557-5.

GEBCO. 2019. General Bathymetric Chart of the Oceans (GEBCO) 2019 grid, doi:10.5285/836f016a-33be-6ddc-e053-6c86abc0788e.

Hirose N, Fukumori I, Zlotnicki V, Ponte RM. 2001. Modeling the high-frequency barotropic response of the ocean to atmospheric disturbances: Sensitivity to forcing, topography, and friction. *Journal of Geophysical Research* 106:30987-30,995, doi:10.1029/2000JC000763.

Hoeke RK, McInnes KL, Kruger JC, McNaught RJ, Hunter JR, Smithers SG. 2013. Widespread inundation of Pacific islands triggered by distant-source wind-waves. *Global and Planetary Change* 108: 128–138, doi:10.1016/j.gloplacha.2013.06.006.

Holman RA, Sallenger AH Jr. 1985. Setup and swash on a natural beach. *Journal of Geophysical Research* 90(C1):945-953, doi:10.1029/JC090iC01p00945.

Hughes CW, Smithson MJ. 1996. Bottom pressure correlations in the south Atlantic. *Geophysical Research Letters* 23(17):2243-2246, doi:10.1029/96GL01319.

IOC. 2002. Manual on sea-level measurement and interpretation. Volume III: Reappraisals and recommendations as of the year 2000.Intergovernmental Oceanographic Commission, Manuals & Guides, No 14, 47pp. & appendices. https://www.psmsl.org/train_and_info/training/manuals/.

IOC. 2012. The Global Sea Level Observing System (GLOSS) Implementation Plan - 2012. UNESCO/Intergovernmental Oceanographic Commission. 48pp. (IOC Technical Series No. 100). Available from https://unesdoc.unesco.org/ark:/48223/pf0000217832.

IOC. 2016. Manual on Sea-level Measurements and Interpretation, Volume V: Radar Gauges. Paris, Intergovernmental Oceanographic Commission of UNESCO. 104pp. (IOC Manuals and Guides No.14, vol. V; JCOMM Technical Report No. 89) (English). https://www.psmsl.org/train_and_info/training/manuals/.

Kalnay E, Kanamitsu M, Kistler R, Collins W, Deaven D, Gandin L, Iredell M, et al. 1996. The NCEP/NCAR 40-year reanalysis project. *Bulletin of the American Meteorological Society* 77:437–470, doi:10.1175/1520-0477(1996)077<0437:TNYRP>2.0.CO;2.

Kieviet J, Bouton P, Van Eeden F. 2016. Physical modelling of emergency repairs to the main breakwater of Calshot Harbour on Tristan da Cunha island. Proceedings of the 6th International Conference on the Application of Physical Modelling in Coastal and Port Engineering and Science (Coastlab16), Ottawa, Canada, May 10-13, 2016. 10pp.

Kim SY, Yasuda T, Mase H. 2010. Wave set-up in the storm surge along open coasts during Typhoon Anita. *Coastal Engineering* 57:631-642, doi:10.1016/j.coastaleng.2010.02.004.

Kistler R, Kalnay E, Collins W, Saha S, White G, Woollen J, Chelliah M, et al. 2001. The NCEP-NCAR 50 year reanalysis: Monthly means CD-ROM and documentation. *Bulletin of the American Meteorological Society* 82:247-267, doi:10.1175/1520-0477(2001)082<0247:TNNYRM>2.3.CO;2.

Longuet-Higgins MS, Stewart RW. 1962. Radiation stress and mass transport in gravity waves, with applications to “surf beats”. *Journal of Fluid Mechanics* 13 :481–504, doi:10.1017/S0022112062000877.

Mehta AJ. 1990. Significance of bay superelevation in measurement of sea level change. *Journal of Coastal Research* 6(4):801-813. Available from http://www.jstor.org/stable/4297751.

Melet A, Almar R, Meyssignac B. 2016. What dominates sea level at the coast: a case study for the Gulf of Guinea. *Ocean Dynamics* 66:623–636, doi:10.1007/s10236-016-0942-2.

McDougal WG, Slotta LS. 1981. Comment on “Wave setup of harbor water levels” by R.O.R.Y. Thompson and B.V. Hamon. *Journal of Geophysical Research Oceans* 86:4309-4310, doi:10.1029/JC086iC05p04309.

Munk WH, Sargent MC. 1948. Adjustment of Bikini Atoll to ocean waves. *EOS, Transactions of the American Geophysical Union* 29(6):855-860, doi:10.1029/TR029i006p00855.

Pedreros R, Idier D, Muller H, Lecacheux S, Paris F, Yates-Michelin M, Dumas F, Pineau-Guillou L, Sénéchal N. 2018. Relative contribution of wave setup to the storm surge: observations and modeling based analysis in open and protected environments (Truc Vert beach and Tubuai island). *Journal of Coastal Research* Special Issue 85:1046–1050, doi:10.2112/SI85-210.1.

Pugh DT, Woodworth PL. 2014. *Sea-level science: Understanding tides, surges, tsunamis and mean sea-level changes.* Cambridge: Cambridge University Press. 408pp.

Spencer R, Foden PR, McGarry C, Harrison AJ, Vassie JM, Baker TF, Smithson MJ, Harangozo SA, Woodworth PL. 1993. The ACCLAIM programme in the South Atlantic and Southern Oceans. *International Hydrographic Review* 70:7-21.

Stockdon HF, Holman RA, Howd PA, Sallenger AH Jr. 2006. Empirical parameterization of setup, swash, and runup. *Coastal Engineering* 53:573-588, doi:10.1016/j.coastaleng.2005.12.005.

Tait RJ. 1972. Wave set-up on coral reefs. *Journal of Geophysical Research* 77(12):2207-2211, doi:10.1029/JC077i012p02207.

TdCG/RSPB. 2012. Biodiversity action plan for the Tristan da Cunha islands (2012-2016). Prepared by the Tristan da Cunha Government and the Royal Society for the Protection of Birds. Tristan Conservation Department, Edinburgh of the Seven Seas, Tristan da Cunha, South Atlantic. 77pp.

Thompson R, Hamon BV. 1980. Wave setup of harbor water levels. *Journal of Geophysical Research* 85(C2):1151-1152, doi:10.1029/JC085iC02p01151.

Thompson R. 1983. Set-up of Sydney Harbour by waves, winds and atmospheric pressure. *Australian Journal of Marine and Freshwater Research* 34:97-103.

Vetter O, Becker JM, Merrifield MA, Pequignet A-C, Aucan J, Boc SJ, Pollock CE. 2010. Wave setup over a Pacific Island fringing reef. *Journal of Geophysical Research* 115:C12066, doi:10.1029/2010JC006455.

Wessel P, Smith WHF. 1998. New, improved version of generic mapping tools released. *EOS Transactions of the American Geophysical Union* 79:579-579.

Woodworth PL, Vassie JM, Spencer R, Smith DE. 1996. Precise datum control for pressure tide gauges. *Marine Geodesy* 19(1):1-20.

Woodworth PL, Le Provost C, Rickards LJ, Mitchum GT, Merrifield M. 2002. A review of sea-level research from tide gauges during the World Ocean Circulation Experiment. *Oceanography and Marine Biology: An Annual Review* 40:1-35.

Woodworth PL, Melet A, Marcos M, Ray RD, Wöppelmann G, Sasaki YN, Cirano M, Hibbert A, Huthnance JM, Montserrat S, Merrifield MA. 2019. Forcing factors affecting sea level changes at the coast. *Surveys in Geophysics* 40:1351-1397, doi:10.1007/s10712-019-09531-1.

Wunsch C, Stammer D. 1997. Atmospheric loading and the oceanic “inverted barometer” effect. *Reviews of Geophysics* 35:79-107, doi:10.1029/96RG03037.

Figure Captions

1.(a) Schematic map of Tristan da Cunha indicating the 500 m depth contour (red) adapted from GEBCO (2019) and with blue dots showing the larger areas of shallower coastal waters (typically < 20 m) inferred from the limited amount of bathymetric information in nautical charts. The red square indicates the settlement of Edinburgh of the Seven Seas and the Tristan harbour at the western end of the north coast. Land areas shown in green are below 100m elevation; otherwise the land rises steeply to the 2062 m summit of the volcano. (Topographic information courtesy of the University of Luxembourg.) (b) Part of a bathymetric chart in the area of the harbour at Tristan da Cunha (north at the top) compiled by WSP/Parsons Brinckerhoff in 2010. The depth contours of 2.5 m, 5 m etc. depths, which are nominally with respect to Lowest Astronomical Tide, are indicated on the left and right. The inner harbour is approximately 65 m (east-west) and 35 m (north-south) wide.

2. (a) The west side of the harbour in February 1992 looking north towards the RMS St. Helena (Photograph: Philip Woodworth). At this time the harbour was roughly circular. (b) An aerial view of Edinburgh of the Seven Seas and Calshot Harbour, looking south, in October 2013 taken from the helicopter of the frigate HMS Richmond (from https://www.tristandc.com/harbour.php). The western extension to the breakwater can be clearly seen. (c) The harbour looking approximately north-west on 19 August 2011 when no fishing was possible and all boats were out of the water (Photograph: Katrine Herian, RSPB). The tide gauges mentioned in this report were deployed at the same location on the east (right) side of the harbour where the cantilever arm of an OTT radar gauge can be just about seen in (c).

3. Time series of 10-hourly residuals of SSP from three BPRs around Tristan da Cunha during 1986-1987 (denoted BPRs) compared to the corresponding values measured by a pressure sensor tide gauge (denoted TG) located in the island harbour. Time series have had their mean values subtracted and are plotted with offsets for presentation purposes as shown by the dashed lines. The three BPRs were deployed approximately 200 km from Tristan da Cunha, at locations approximately to the NE (red), W (blue) and SE (green) of the island, in depths of 4100, 3500 and 3100 m respectively.

4. Time series of 10-hourly residuals of SSP from a series of island harbour tide gauges at Tristan da Cunha between 1986-1997 with the end of each individual record indicated by a triangle. The average of the residuals over each individual record has been subtracted from the individual 10-hourly values. For comparison, the blue curve shows DAC-adjusted sea level (in effect SSP) at Tristan from 1992 obtained from satellite altimetry with the average of that curve adjusted to be the same as that of the tide gauge values over their period in common. The vertical dashed line indicates the pre- and post-1992 sections of data discussed in the text.

5. Time series of daily sea level from radar tide gauges at Tristan da Cunha adjusted for air pressure assuming a static response, thereby providing effectively daily values of SSP (red) compared to DAC-adjusted sea levels from satellite altimetry (blue) with the average of the two adjusted to be the same over their period in common. The two wave setup spikes (on 5-6 July 2011 and 19 May 2012) discussed in the text propagate into the tide gauge daily SSP values on those days. The altimeter data are 7-day means derived from the 'reference series' of missions.

6. The difference between the sea level response to air pressure and winds at Tristan obtained from the DAC model and the simple IB response to air pressure changes during 1993-1997.

7. An explanation of the reason for similarity between spikes in the 1-hour and 10-residuals. The red line shows 1-hour residuals centred on the time of a large positive spike in the 10-hour residuals, the

10-hour residual of the spike indicated by the blue star. The 10-hour residual is less than the maximum 1-hour residual, but not to any great extent, owing to the wave setup event lasting for an extended period.

8. (a) Six-hourly significant wave height at Tristan during 1986-1992 obtained from the ERA-Interim reanalyses of ECMWF, (b) wave direction (the direction from which waves arrive measured clockwise from north), and (c) wave period. (d-f) As for figures (a-c) selecting only those occasions when there were positive spikes in the 1-hour tide gauge residuals larger than 25 cm (or 25 mbar in terms of SSP).

9. (a) A histogram of all tide gauge residuals during 1986-1992, and (b) a histogram of 5% of the residuals, selecting large waves (SWH > 4 m) and from the northerly direction (direction 270° - 45°).

10. (a) Significant wave height at Tristan da Cunha during 2011-2013, the period when radar tide gauges were operated at Tristan. (b) Wave direction, and (c) wave period. The black curves show annual fits in each case.

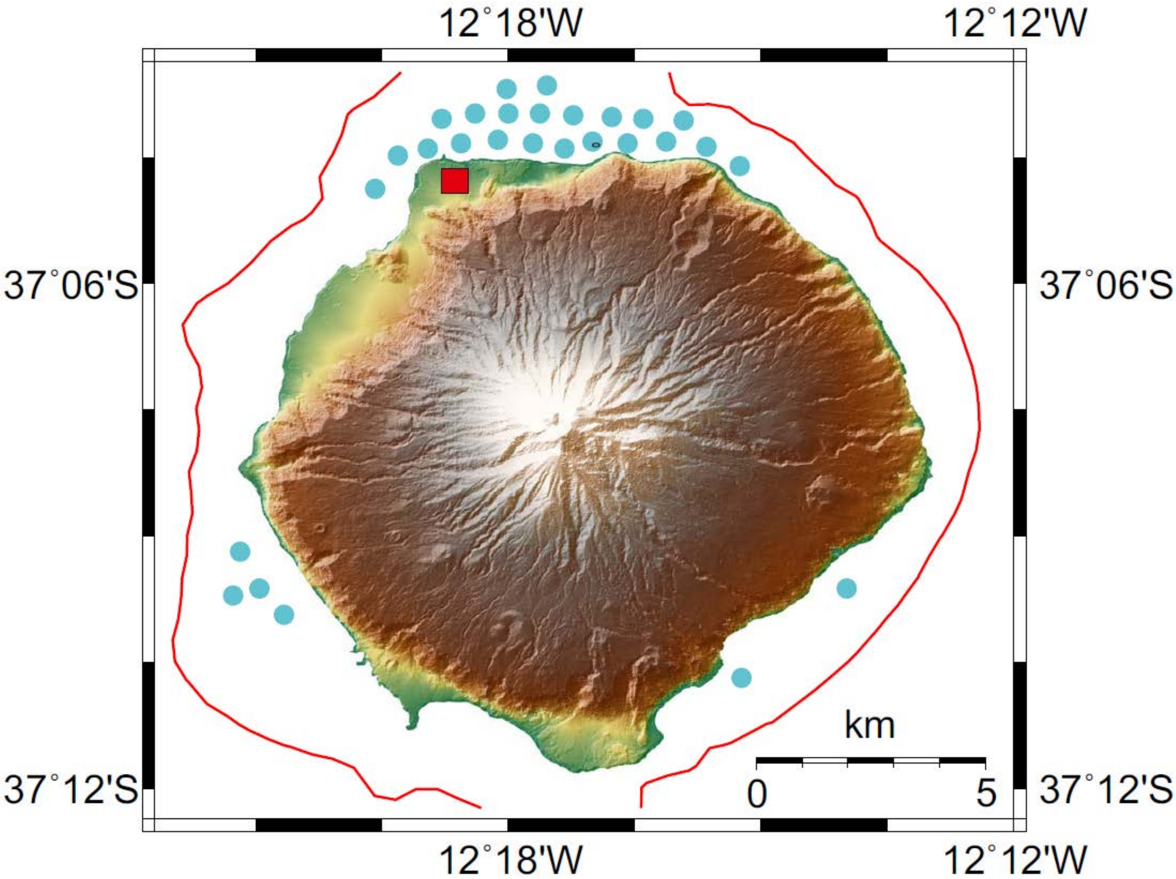

Figure 1a

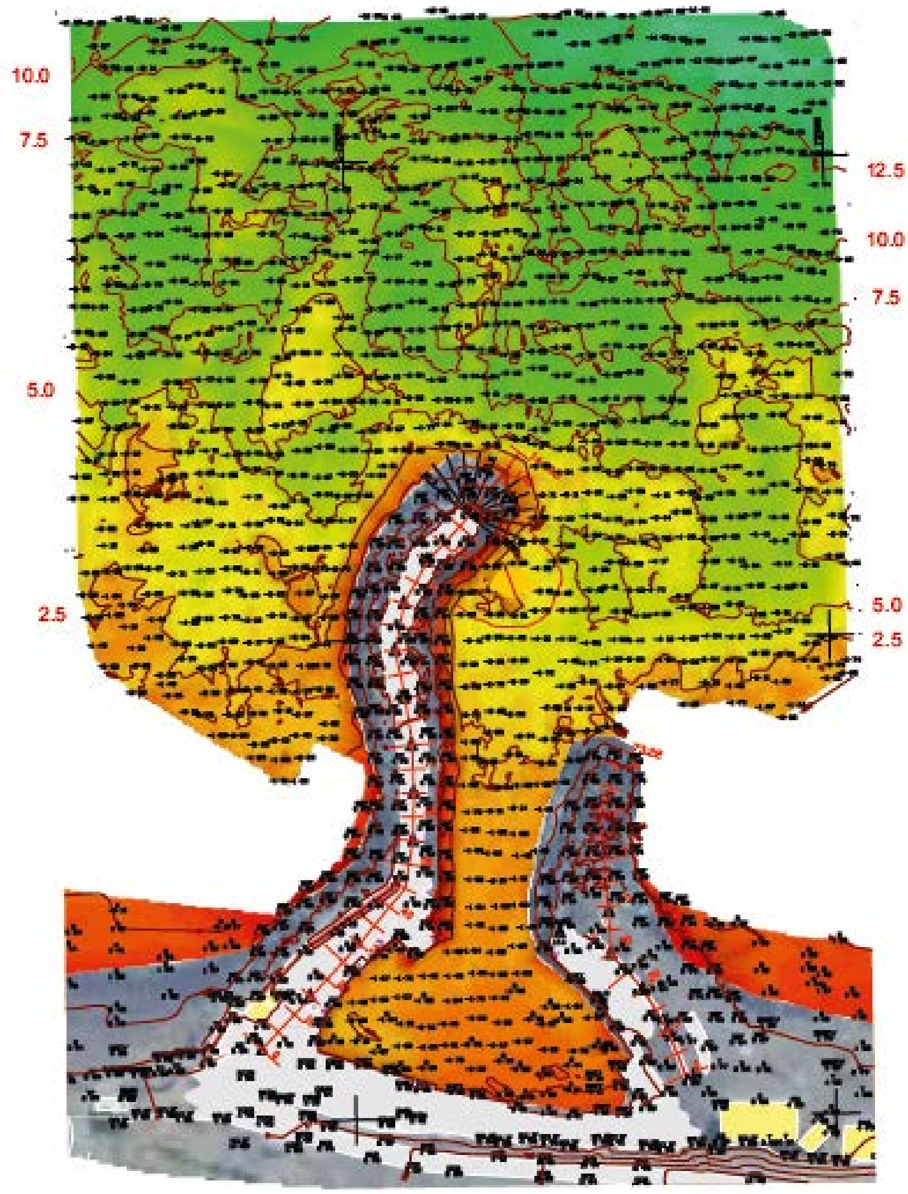

Figure 1b

Figure 2a

Figure 2b

Figure 2c

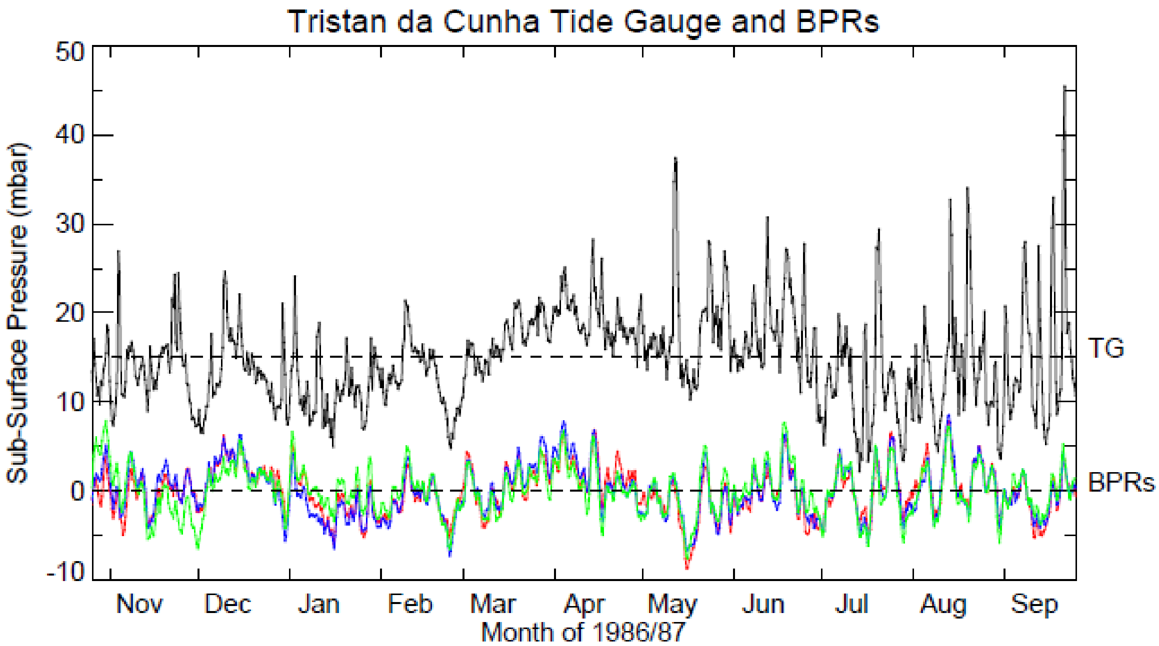

Figure 3

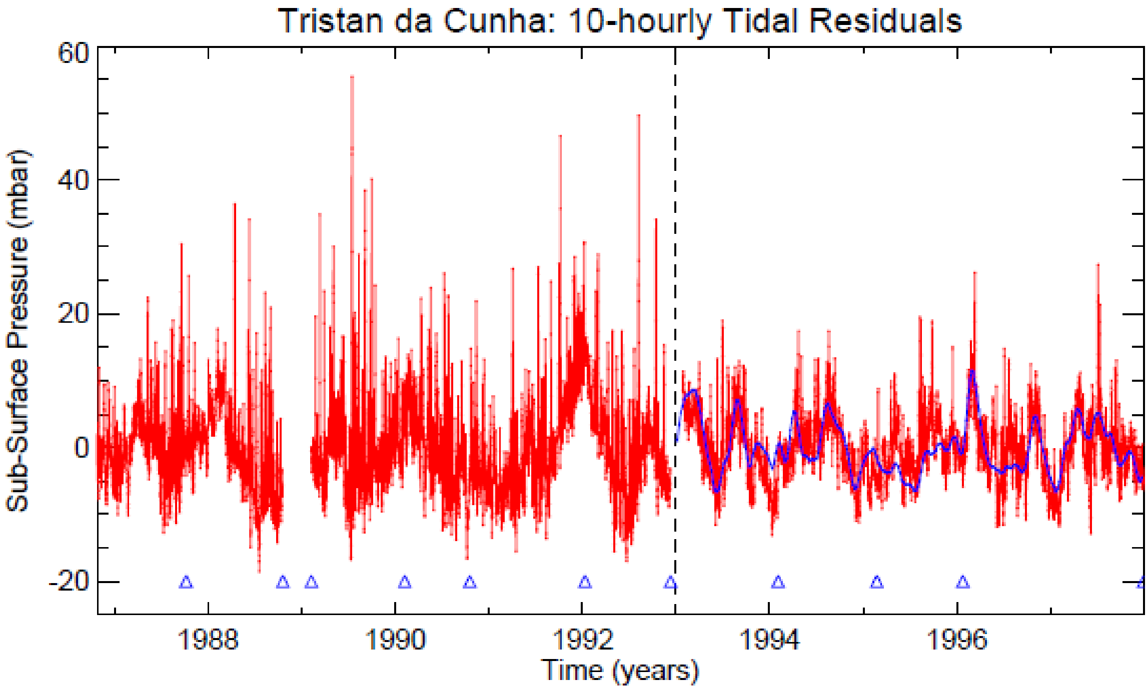

Figure 4

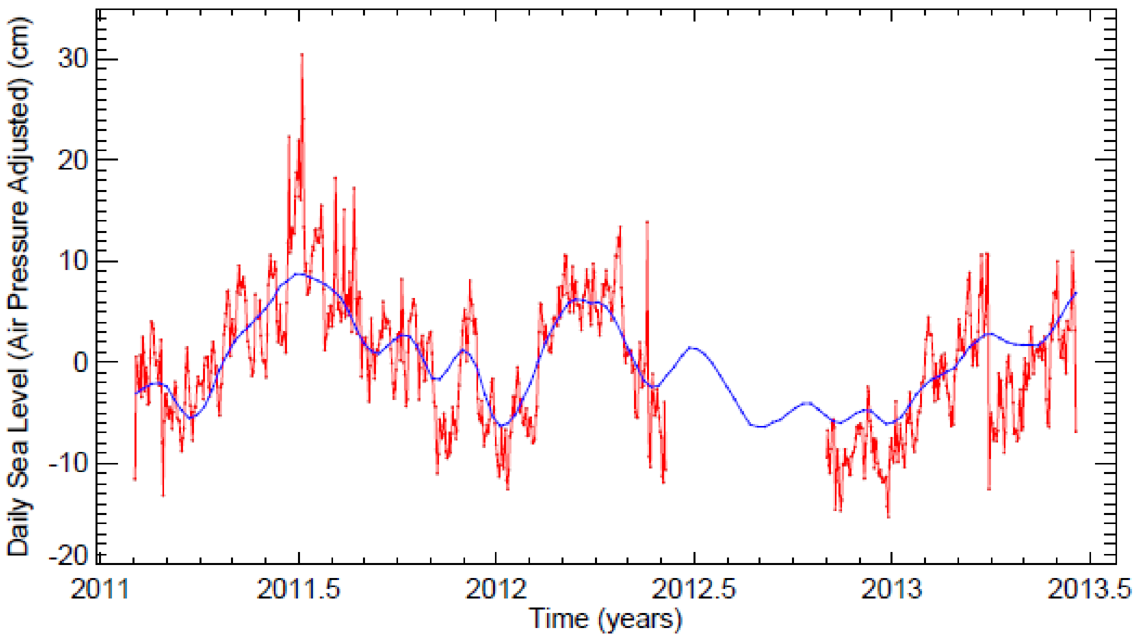

Figure 5

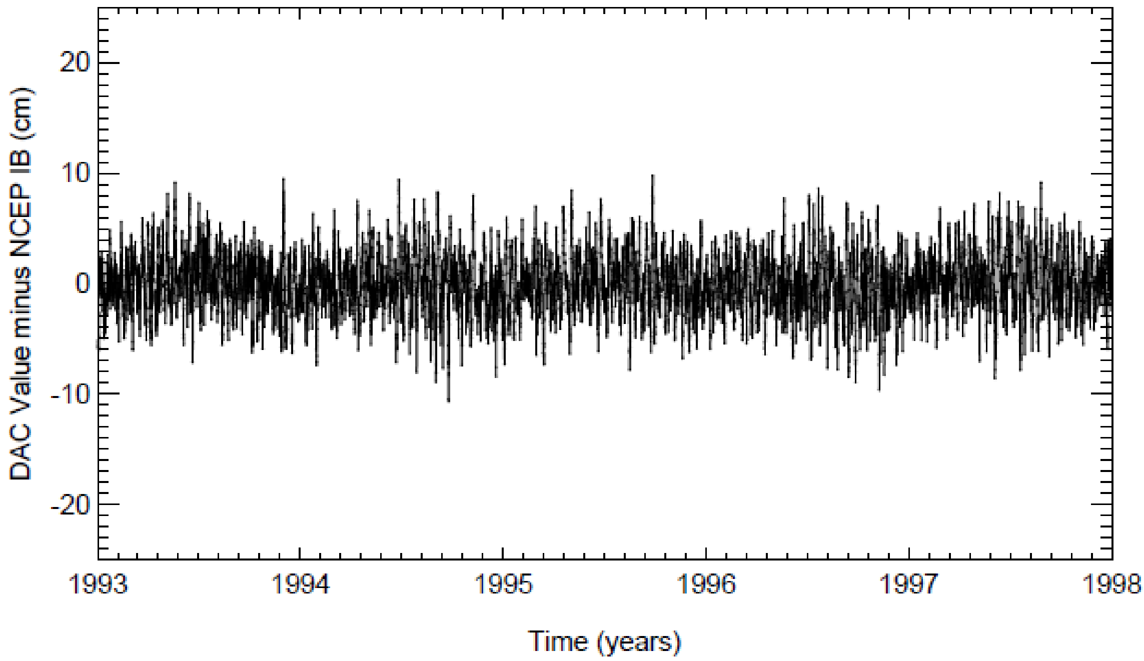

Figure 6

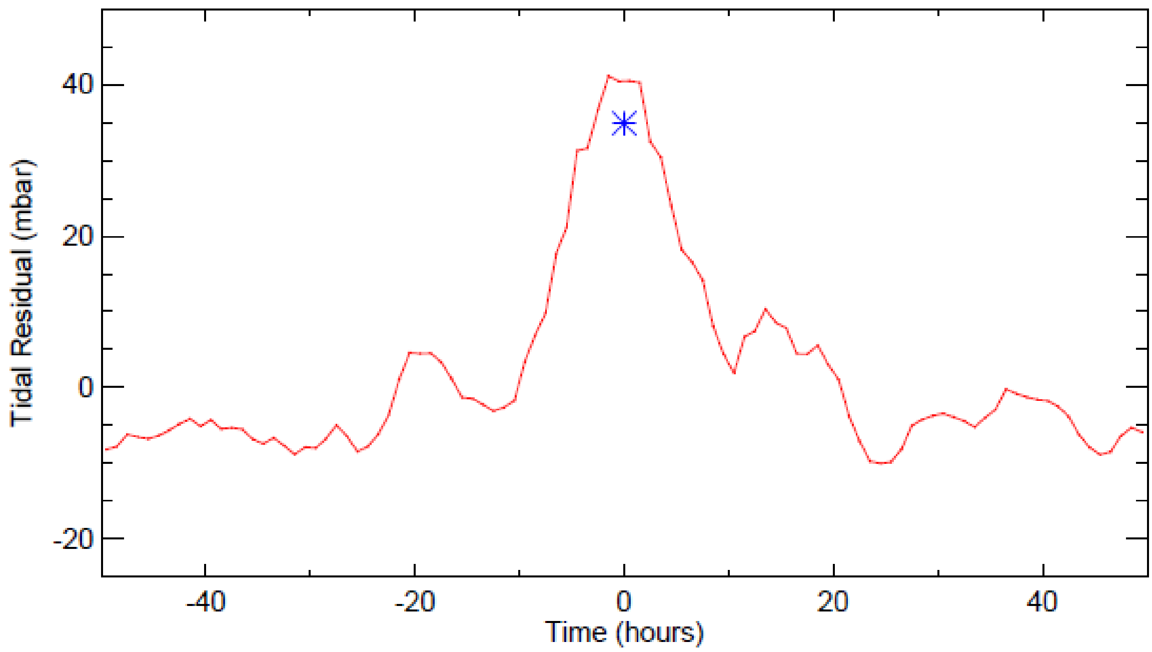

Figure 7

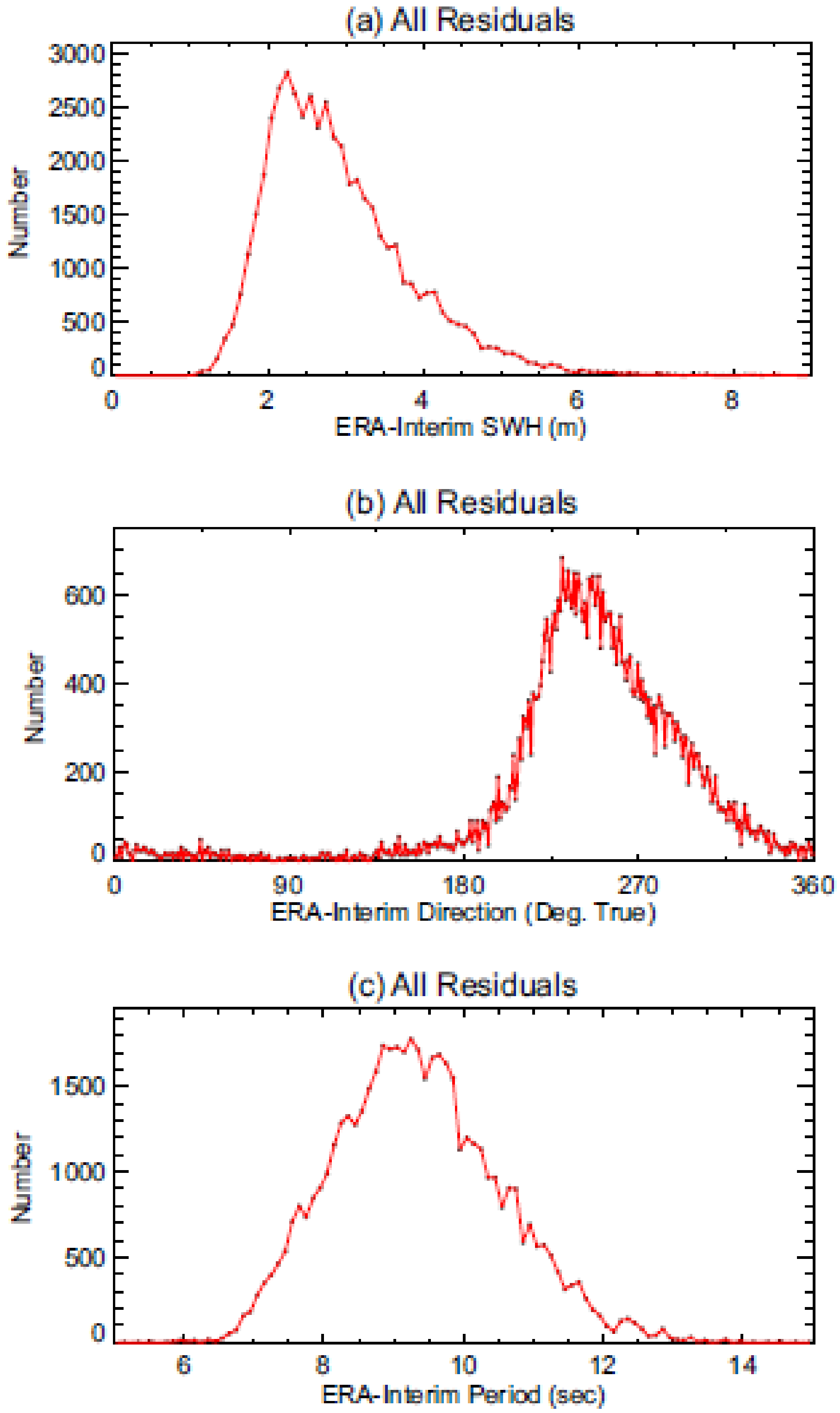

(a) All Residuals
Number
3000
2500
2000
1500
1000
500
0
0
2
4
6
8
ERA-Interim SWH (m)
(b) All Residuals
Number
600
400
200
0
0
90
180
270
360
ERA-Interim Direction (Deg. True)
(c) All Residuals
Number
1500
1000
500
0
6
8
10
12
14
ERA-Interim Period (sec)

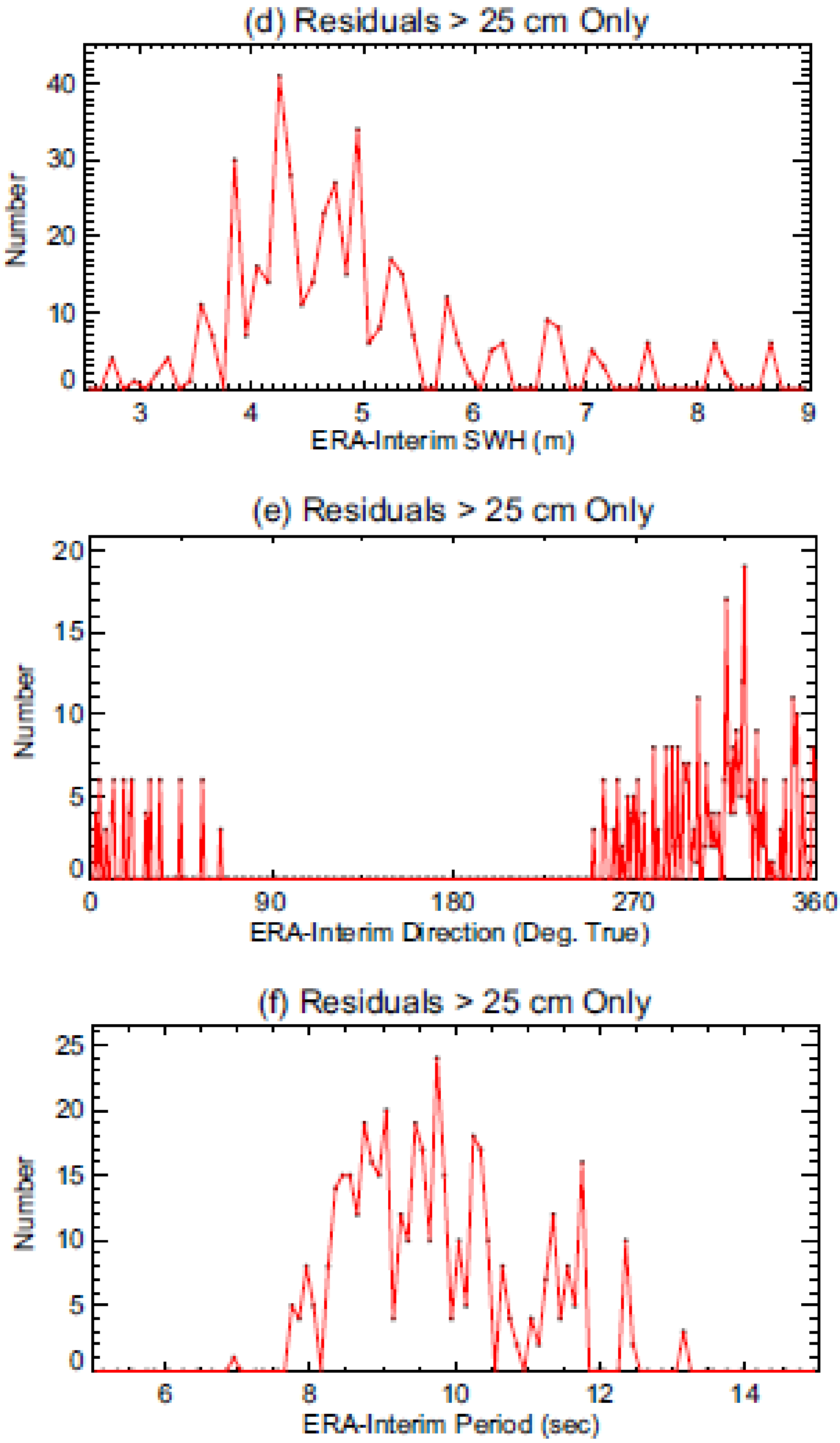
(d) Residuals > 25 cm Only
Number
40
30
20
10
0
3
4
5
6
7
8
9
ERA-Interim SWH (m)
(e) Residuals > 25 cm Only
Number
20
15
10
5
0
0
90
180
270
360
ERA-Interim Direction (Deg. True)
(f) Residuals > 25 cm Only
Number
25
20
15
10
5
0
6
8
10
12
14
ERA-Interim Period (sec)

Figure 8

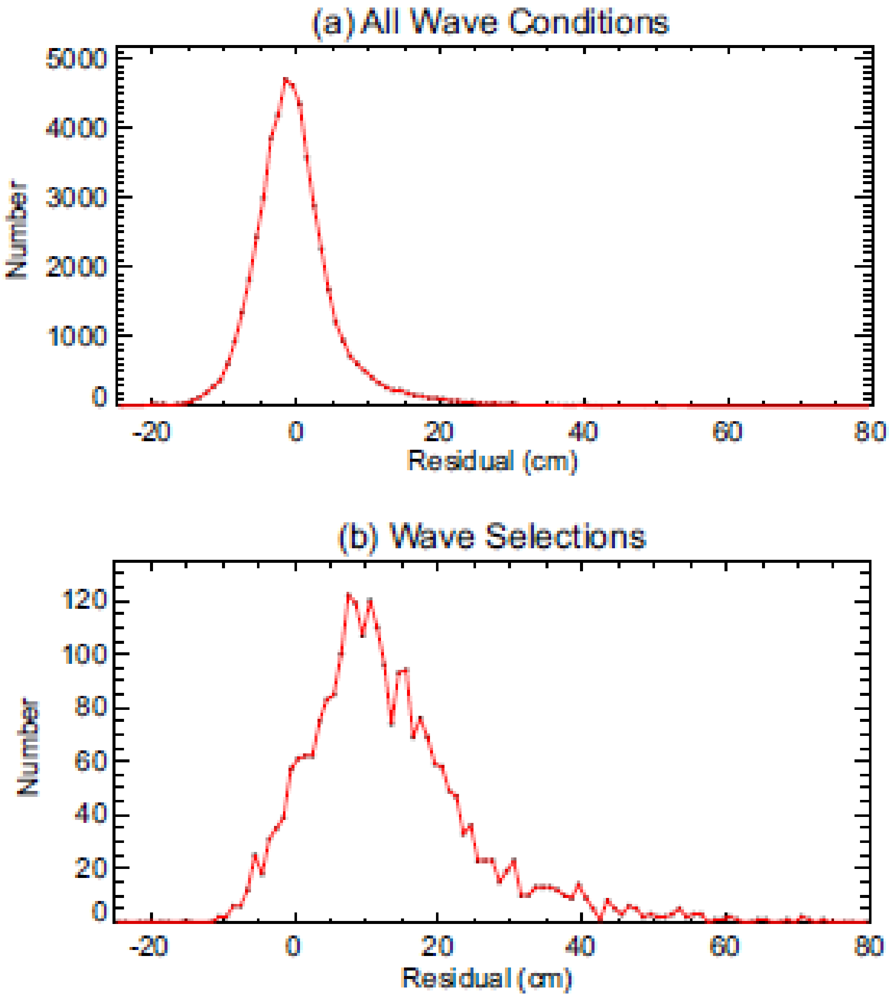
(a) All Wave Conditions
Number
Residual (cm)
(b) Wave Selections
Number
Residual (cm)

Figure 9

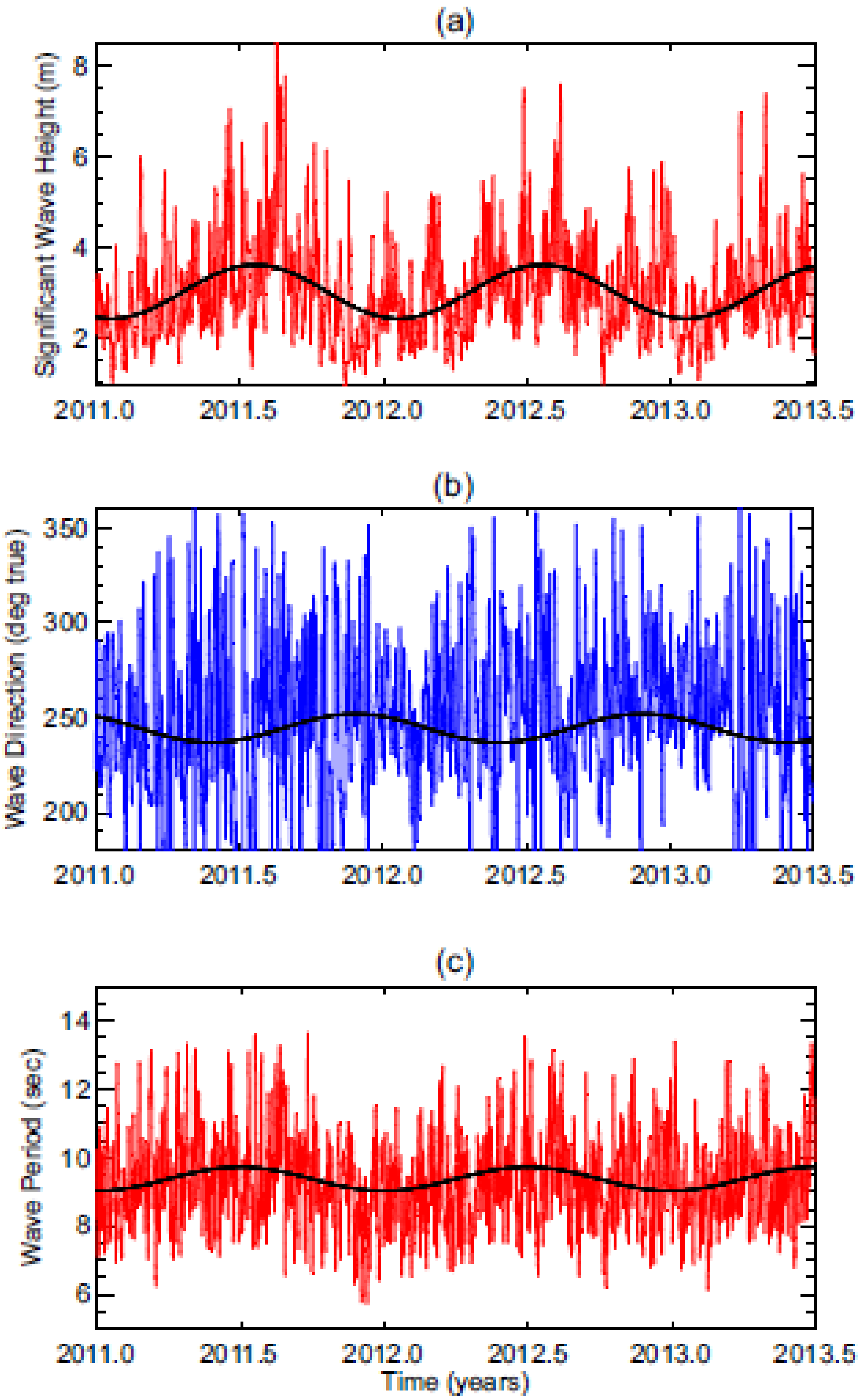
(a)
Significant Wave Height (m)
8
6
4
2
2011.0
2011.5
2012.0
2012.5
2013.0
2013.5
(b)
Wave Direction (deg true)
350
300
250
200
2011.0
2011.5
2012.0
2012.5
2013.0
2013.5
(c)
Wave Period (sec)
14
12
10
8
6
2011.0
2011.5
2012.0
2012.5
2013.0
2013.5
Time (years)

Figure 10